

## Supplementary Information

### **A novel copper formate-based framework $\text{RbCu}(\text{HCO}_2)_2\text{Cl}$ : synthesis, crystal structure, thermal, vibrational and magnetic properties and antibacterial activity**

Asmae Ben Abdelhadi,<sup>a,b</sup> Safaa Hidaoui,<sup>a</sup> Rachid Ouarsal,<sup>a</sup> Morgane Poupon,<sup>c</sup> Michal Dusek,<sup>c</sup> María de los Llanos Palop Herreros,<sup>d</sup> Marco Antonio López de la Torre,<sup>e</sup> Luis Lezama,<sup>f</sup> Brahim El Bali,<sup>a</sup> Mohammed Lachkar\*<sup>a</sup> and Abderrazzak Douhal\*<sup>b</sup>.

<sup>a</sup>Engineering Laboratory of Organometallic, Molecular Materials, and Environment (LIMOME), Faculty of Sciences, Sidi Mohamed Ben Abdellah University, 30000 Fez, Morocco.

<sup>b</sup>Departamento de Química Física, Facultad de Ciencias Ambientales y Bioquímica, e INAMOL, Campus Tecnológico de Toledo, Universidad de Castilla-La Mancha (UCLM), Avenida Carlos III, S.N., 45071 Toledo, Spain.

<sup>c</sup>Institute of Physics of the Czech Academy of Sciences, Na Slovance 2, 8, Praha 182 21, Czech Republic.

<sup>d</sup>Departamento de Química Analítica y Tecnología de los Alimentos, Facultad de Ciencias Ambientales y Bioquímica, Universidad de Castilla-La Mancha, (UCLM), Avenida Carlos III, S.N., 45071 Toledo, Spain.

<sup>e</sup>Departamento de Física, Facultad de Ciencias Ambientales y Bioquímica, and INAMOL, Universidad de Castilla-La Mancha, Avenida Carlos III, S.N., 45071 Toledo, Spain.

<sup>f</sup>Departamento de Química Orgánica e Inorgánica, Facultad de Ciencia y Tecnología, Universidad del País Vasco, UPV/EHU, Bº Sarriena s/n, 48940 Leioa, Spain.

\*Corresponding authors: [mohammed.lachkar@usmba.ac.ma](mailto:mohammed.lachkar@usmba.ac.ma) (M. L.) & [Abderrazzak.Douhal@uclm.es](mailto:Abderrazzak.Douhal@uclm.es) (A. D.)

## Index

**Evaluation of Antibacterial Activity** Page 3

**Table S1.** Fractional atomic coordinates and isotropic or equivalent isotropic displacement parameters ( $\text{\AA}^2$ ) for  $\text{RbCu}(\text{HCO}_2)_2\text{Cl}$ . Page 5

**Table S2.** Atomic displacement parameters ( $\text{\AA}^2$ ) for  $\text{RbCu}(\text{HCO}_2)_2\text{Cl}$ . Page 5

**Table S3.** IR absorption bands ( $\text{cm}^{-1}$ ) and their assignments for  $\text{RbCu}(\text{HCO}_2)_2\text{Cl}$  (Relative intensities: vs, very strong; s; strong, m: medium; w: weak; vw: very weak; sh: shoulder; br: broad). Page 6

**Figure S1.** Typical synthesis procedure for synthesizing  $\text{RbCu}(\text{HCO}_2)_2\text{Cl}$  single crystal using a facile slow diffusion process (A). Optical photograph of the as-prepared **1** single crystal in the daylight (B). Page 6

**Figure S2.** HR-MS spectrum of  $\text{RbCu}(\text{HCO}_2)_2\text{Cl}$ . Page 7

**Figure S3.** Field-dependent magnetization of  $\text{RbCu}(\text{HCO}_2)_2\text{Cl}$  at 5 K. Page 7

**Figure S4.** Thermal evolution of the X-band EPR spectra of a powder sample. Page 8

**Figure S5.** Experimental and simulated X-band EPR spectra of  $\text{RbCu}(\text{HCO}_2)_2\text{Cl}$  at 5 K (see text for details of fit). Page 8

**Figure S6.** Inhibition of halo diameters from disc and agar well diffusion methods obtained for *S. aureus* CECT 86 (A); *L. monocytogenes* CECT 4031 (B), *E. coli* CECT 99 (C) and *K. pneumoniae* CECT 143<sup>T</sup> (D). Page 9

**Acknowledgments** Page 9

**References** Page 9

**Evaluation of Antibacterial Activity.**  $\text{RbCu}(\text{HCO}_2)_2\text{Cl}$  was assayed for its antibacterial activity against four potentially pathogenic bacteria: two Gram-positive bacteria, *S. aureus* CECT 86 and *L. monocytogenes* CECT 4031 and two Gram-negative bacteria, *E. coli* CECT 99 and *K. pneumoniae* CECT 143<sup>T</sup>. All of them were purchased from the Colección Española de Cultivos Tipo (CECT). These bacteria were maintained frozen (-80 °C) with 20% (v/v) glycerol and they were revitalized by cultivation in Tryptone Soy Broth (TSB) (*S. aureus*, *E. coli* and *K. pneumoniae*) or Brain Heart Infusion (BHI) broth (*L. monocytogenes*) and incubated under static conditions at 37 °C for 24 h.

A phenotypic assay by using both the disc diffusion method<sup>1</sup> and the agar well diffusion method<sup>2</sup> was carried out. Cells from overnight cultures of the strains in TSB or BHI broth were harvested by centrifugation at 18,500 x g for 5 min at 4 °C and suspended in sterile phosphate buffer saline (PBS) pH 7.2 to reach the 0.5 McFarland turbidity standard, equivalent to 10<sup>8</sup> colony-forming units (CFU)/mL. These suspensions were smeared on Mueller-Hinton (Pronadisa, Madrid, Spain) agar (MHA) plates by using a sterile cotton swab and allowed to dry for 10 min.

For the disc diffusion method, 6 mm blank discs (Oxoid, Hampshire, UK) were used which were spotted with 20 µL of a sterile 15 mg/mL solution of compound **1** in distilled water. Millex-GV 0.22 µm filters were used for sterilization. On the same plate, discs containing antibiotics able to inhibit growth of each of the bacteria assayed were also overlaid as a control. For *S. aureus* CECT 86 the antibiotics norfloxacin (5 µg) and vancomycin (30 µg) were used; for *L. monocytogenes* CECT 4031, gentamicin (10 µg) and ampicillin- sulfactam (10/10 µg); for *E. coli* CECT 99 trimethoprim-sulfamethoxazole (25 µg) and nitrofurantoin (300 µg) and for *K. pneumoniae* CECT 143<sup>T</sup> ciprofloxacin (5 µg) and gentamicin (10 µg). All were purchased from Bio-Rad (Marnes-la Coquette, France).

For the agar well diffusion method, MHA plates were smeared as described for the disc diffusion test and wells of 6 mm of diameter were bored on the surface of the agar. 20  $\mu$ L of the same solution used for the disc diffusion test were added to the wells. Plates from both assays were incubated at 37 °C for 24 h and then the inhibition halos (diameter in mm) were recorded. Both assays were performed in duplicate.

In addition, a quantitative assay to determine the MIC (Minimum Inhibitory Concentration) was carried out by using 96-well microtiter plates. Concentrations of the compound **1** between 400  $\mu$ g/mL and 2500  $\mu$ g/mL were assayed by adding to each well a volume of the culture medium (TSB or BHI broth) and the adequate volume of the sterile 15 mg/mL solution of the compound to reach the desired concentration. All the wells were inoculated with 20  $\mu$ L of an overnight culture of the strain assayed. The final volume in wells was 200  $\mu$ L. Blanks without inoculum were also prepared to confirm the maintenance of sterility of both the culture medium and the solution of compound **1** during incubation. In addition, cultures of each of the strains in the culture medium in absence of the compound were prepared. Assays were performed by triplicate. Microtiter plates were incubated at 37 °C during 24 h in the reader Synergy HT (Biotek, EEUU), and the growth during incubation was monitored by measurement of the optical density at 600 nm ( $OD_{600}$ ) in the wells every 30 min, previous gentle stirring.

To determine the cell population in the overnight culture of the strain used as inoculum and that in the wells after the incubation, a viable cell count was carried out. 10  $\mu$ L of serial dilutions of the cultures in sterile saline solution (9.5 g/L w/v) were plated onto TSA or BHIA plates by triplicate. After incubating the plates for 24 h at 37°C, the colonies were counted, and the results were expressed as CFU/mL of culture. The decrease of growth in percentage from each concentration of compound **1** assayed was calculated with respect to the counts obtained in the cultures in the absence of the compound.

**Table S1.** Fractional atomic coordinates and isotropic or equivalent isotropic displacement parameters ( $\text{\AA}^2$ ) for  $\text{RbCu}(\text{HCO}_2)_2\text{Cl}$ .

	<i>x</i>	<i>y</i>	<i>z</i>	$U_{\text{iso}}^*/U_{\text{eq}}$
Rb1	-0.01499 (4)	0.52896 (4)	0.26858 (3)	0.03449 (12)
Cu2	0.38405 (4)	0.61818 (5)	0.51068 (3)	0.02161 (12)
Cl1	0.16548 (9)	0.79632 (10)	0.56700 (8)	0.0322 (2)
O1	-0.2490 (2)	0.5895 (3)	0.4757 (2)	0.0305 (7)
O2	0.3428 (3)	0.6045 (3)	0.3089 (2)	0.0333 (7)
O3	0.4710 (3)	0.5987 (3)	0.7056 (2)	0.0315 (7)
O4	0.5578 (3)	0.7859 (3)	0.4840 (2)	0.0324 (7)
C1	0.4206 (4)	0.5001 (4)	0.2442 (3)	0.0299 (10)
C2	-0.2997 (4)	0.7366 (4)	0.4728 (3)	0.0297 (10)
H1c1	0.394537	0.495467	0.145968	0.0359*
H1c2	-0.220418	0.822152	0.460593	0.0357*

**Table S2.** Atomic displacement parameters ( $\text{\AA}^2$ ) for  $\text{RbCu}(\text{HCO}_2)_2\text{Cl}$ .

	$U^{11}$	$U^{22}$	$U^{33}$	$U^{12}$	$U^{13}$	$U^{23}$
Rb1	0.0328 (2)	0.0356 (2)	0.0355 (2)	-0.00112 (14)	0.00563 (14)	0.00607 (14)
Cu2	0.0222 (2)	0.0209 (2)	0.0219 (2)	0.00037 (14)	0.00264 (14)	0.00013 (14)
Cl1	0.0307 (4)	0.0286 (4)	0.0381 (4)	0.0090 (3)	0.0080 (3)	0.0031 (3)
O1	0.0264 (11)	0.0244 (12)	0.0418 (13)	-0.0044 (9)	0.0089 (10)	-0.0009 (10)
O2	0.0338 (12)	0.0441 (14)	0.0217 (11)	0.0075 (11)	0.0010 (9)	-0.0005 (10)
O3	0.0398 (13)	0.0311 (13)	0.0228 (11)	0.0044 (10)	-0.0021 (10)	0.0006 (9)
O4	0.0306 (12)	0.0224 (12)	0.0452 (13)	-0.0015 (10)	0.0085 (10)	0.0027 (10)
C1	0.0332 (18)	0.0358 (19)	0.0199 (15)	-0.0038 (15)	-0.0016	0.0019 (14)

					(13)	
C2	0.0340 (18)	0.0250 (18)	0.0308 (16)	-0.0102 (14)	0.0058 (14)	-0.0005 (14)

**Table S3.** IR absorption bands ( $\text{cm}^{-1}$ ) and their assignments for  $\text{RbCu}(\text{HCO}_2)_2\text{Cl}$  (Relative intensities: vs, very strong; s; strong, m: medium; w: weak; vw: very weak; sh: shoulder; br: broad).

Wavenumber ( $\text{cm}^{-1}$ )	Assignment
2976 vw, br and 2945 vw, br	$2\nu_4(\text{HCOO}), \nu_4 + \nu_5$
2595 vw and 2845 vw	C-H stretching mode $\nu_1(\text{HCOO})$
1614 s and 1552 s, sh	C–O asymmetric stretching modes $\nu_4(\text{HCOO})$
1413 m, 1386 m and 1376 sh	C-H in-plane bending mode $\nu_5(\text{HCOO})$
1337s	C-O symmetric stretching mode $\nu_2(\text{HCOO})$
1045 w	C–H out-of-plane bending mode $\nu_6(\text{HCOO})$
769m	O-C-O symmetric bending mode $\nu_3(\text{HCOO})$
403m	Cu-O stretch

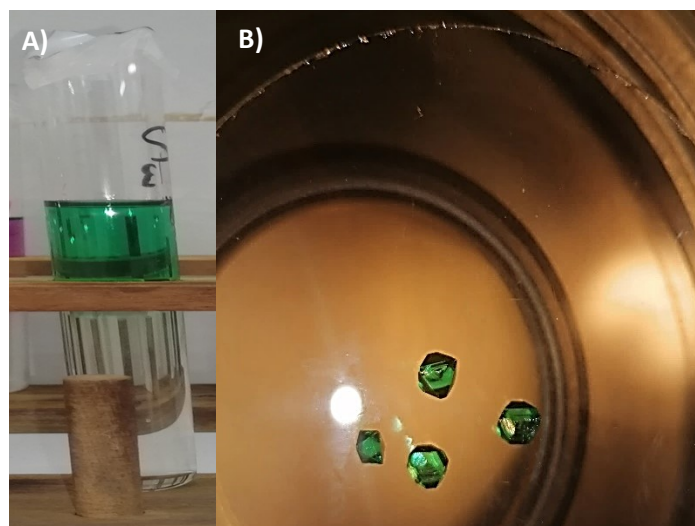


**Figure S1.** Typical synthesis procedure for synthesizing RbCu(HCO<sub>2</sub>)<sub>2</sub>Cl single crystal using a facile slow diffusion process (A). Optical photograph of the as-prepared **1** single crystal in the daylight (B).

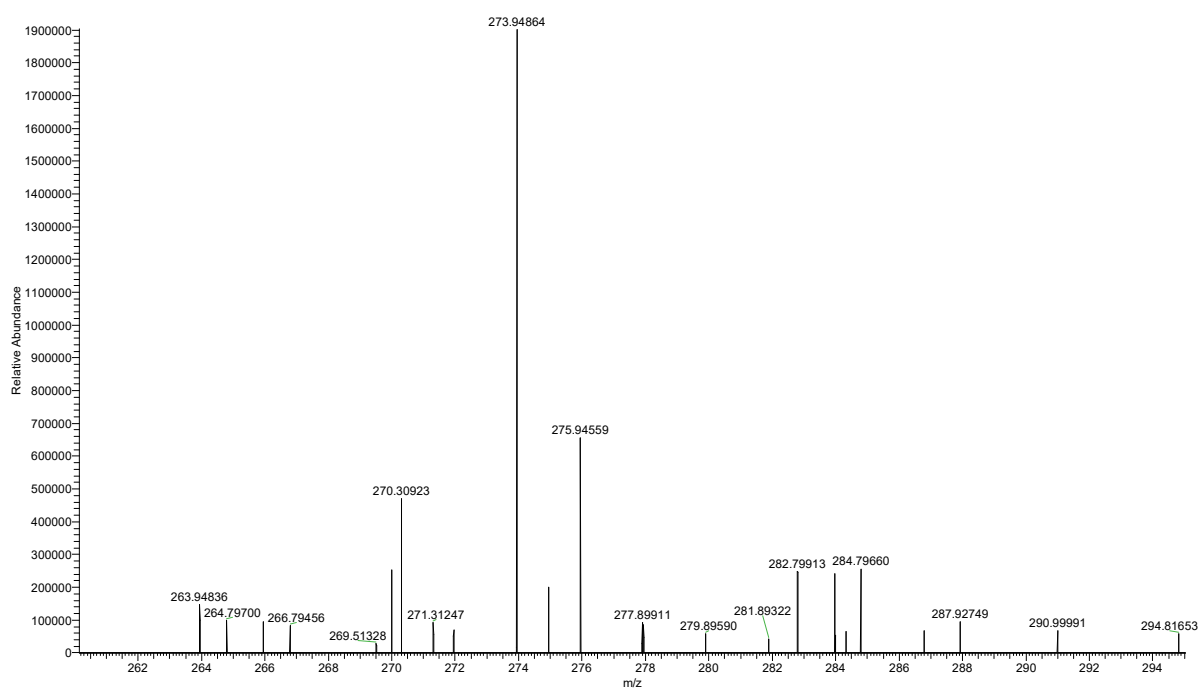


**Figure S2.** HR-MS spectrum of RbCu(HCO<sub>2</sub>)<sub>2</sub>Cl.

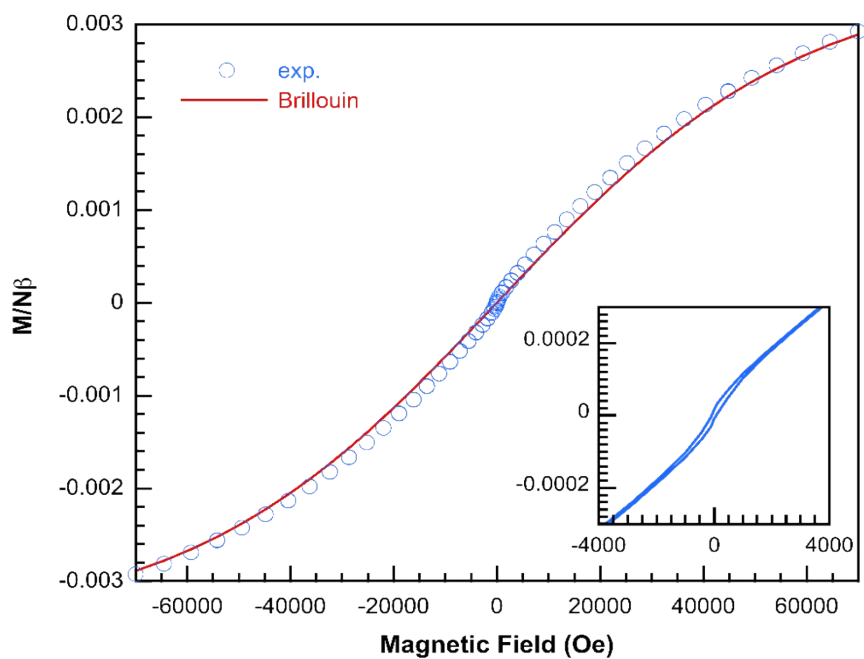


**Figure S3.** Field-dependent magnetization of  $\text{RbCu}(\text{HCO}_2)_2\text{Cl}$  at 5 K.

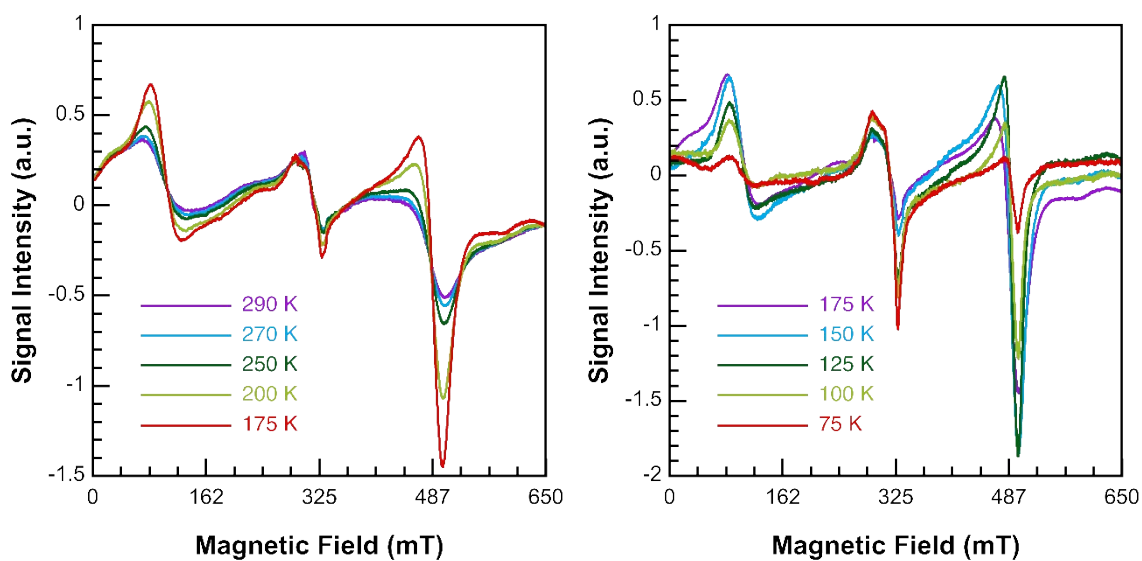


**Figure S4.** Thermal evolution of the X-band EPR spectra of a  $\text{RbCu}(\text{HCO}_2)_2\text{Cl}$  powder sample.



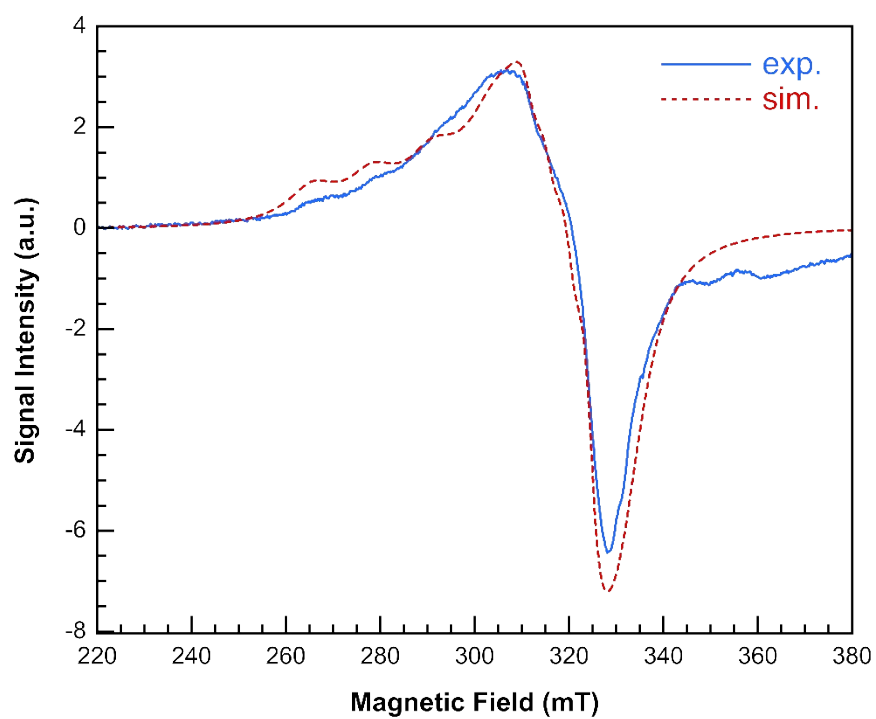


**Figure S5.** Experimental and simulated X-band EPR spectra of  $\text{RbCu}(\text{HCO}_2)_2\text{Cl}$  at 5 K (see text for details of fit).

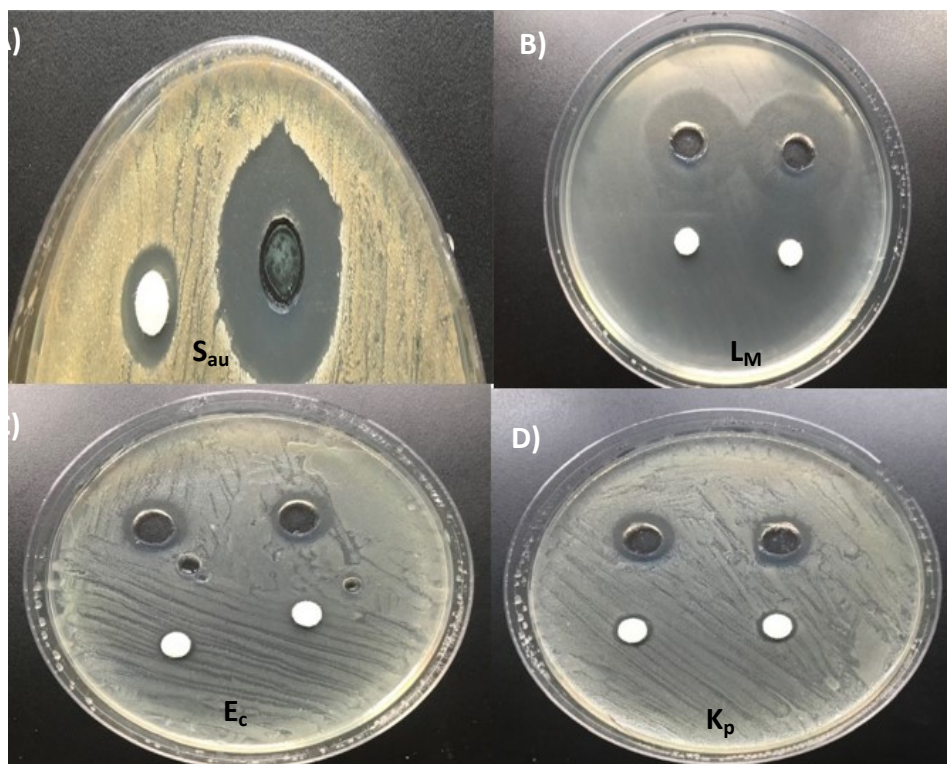


**Figure S6.** Inhibition of halo diameters from disc and agar well diffusion methods obtained for *S. aureus* CECT 86 (A); *L. monocytogenes* CECT 4031 (B), *E. coli* CECT 99 (C) and *K. pneumoniae* CECT 143<sup>T</sup> (D).

### Acknowledgements

This work was supported by the following grants: grant PID2020-116519RB-I00 and TED2021-131650B-I00 funded by MICIU/AEI/10.13039/501100011033 and the European Union (EU). A.B.A. is grateful for the grant from the Spanish Service for the Internationalization of Education (SEPIE), through the EU Erasmus+ key action program (2020-1-ES01-KA107-079868). The authors A. B. A., S. H., R. O., B. E. B. and M. L. would like to acknowledge the technical assistance of the Interface Regional University Center (University Sidi Mohammed Ben Abdellah, Fez, Morocco). Crystallographic analysis was supported by the project 20-LM2023051 of the Czech Nanolab Infrastructures, supported by MEYS CR.

### References

1. H. Fleming, J. Etchells and R. Costilow, *Applied microbiology*, 1975, **30**, 1040-1042.
2. S. Magaldi, S. Mata-Essayag, C. H. De Capriles, C. Pérez, M. Colella, C. Olaizola and Y. Ontiveros, *International journal of infectious diseases*, 2004, **8**, 39-45.